Available online at www.sciencedirect.com

SciVerse ScienceDirect

Nuclear Physics B (Proc. Suppl.) 222–224 (2012) 119–130

NUCLEAR PHYSICS B PROCEEDINGS SUPPLEMENTS

www.elsevier.com/locate/npbps

Inclusive Diffraction at HERA

Mikhail Kapishin for the H1 and ZEUS Collaborations

Joint Institute for Nuclear Research, Joliot Curie 6, 141980 Dubna, Russia

Abstract

Results are reported on measurements of diffractive cross sections in deep-inelastic scattering (DIS) and photoproduction at HERA. The cross sections are compared for processes with a leading proton in the final state and with a large gap in the rapidity distribution of the final state hadrons. The cross section dependences on the proton fractional longitudinal momentum loss $x_{I\!P}$ and the squared four-momentum transfer at the proton vertex t are interpreted in terms of an effective pomeron trajectory and a sub-leading exchange. The hypothesis of proton vertex factorisation is tested. The longitudinal structure function is extracted from the diffractive cross sections measured at different proton beam energies. The cross sections of diffractive dijet production are compared with QCD predictions at next-to-leading order (NLO) based on parton distribution functions obtained from diffractive inclusive DIS data. Combined NLO QCD fits to the inclusive and dijet DIS data are performed to determine diffractive quark singlet and gluon densities with a better precision. The ratio of the diffractive dijet cross sections in photoproduction and DIS is compared with NLO QCD predictions to test QCD collinear factorisation.

Keywords: DIS, HERA, hard diffraction, diffractive parton distribution functions, diffractive dijet production, diffractive longitudinal structure function

1. Introduction

Diffractive processes such as $ep \to eXp$ have been studied extensively in deep-inelastic electron-proton scattering (DIS) at the HERA collider [1, 2, 3, 4, 5, 6]. Their understanding at a fundamental level is crucial for the development of quantum chromodynamics (QCD) at high energies.

The photon virtuality Q^2 provides a hard scale for perturbative QCD to be applicable, so that diffractive DIS events can be viewed as processes in which the photon probes a net colour singlet combination of exchanged partons. The structure of the colour singlet can be studied using a QCD approach based on the hard scattering collinear factorisation theorem [7]. It states that at fixed $x_{I\!P}$, the proton's fractional longitudinal momentum loss, and t, the squared four-momentum transfer at the proton vertex, the diffractive cross section is given by the product of diffractive proton parton distribution functions f_i^D and the partonic hard scattering cross sections $\sigma^{\gamma^* i}$:

$$\sigma_r^{D(4)} \sim \sum \sigma^{\gamma^* i}(x, Q^2) \otimes f_i^D(x, Q^2, x_{I\!P}, t)\,, \qquad (1)$$

where f_i^D are universal for diffractive ep DIS processes (inclusive, dijet and charm production) and obey the DGLAP evolution equations, and $\sigma^{\gamma^* i}$ are the same as for inclusive DIS. This approach allows us to test the diffractive exchange within the perturbative QCD framework and extract 'diffractive parton distribution functions' (DPDFs). The DPDFs can be applied to the analysis of boson-gluon fusion processes of dijet and charm production, where the p_T of jets and the mass of the charm quark provide hard scales and enable perturbative QCD to be applied to the data. These processes are directly sensitive to the gluon density in the colour singlet.

Within Regge phenomenology, diffractive cross sections at low $x_{I\!P}$ are described by the exchange of a pomeron ($I\!P$) trajectory. Diffractive DIS cross sections

0920-5632/$ – see front matter
doi:10.1016/j.nuclphysbps.2012.03.013

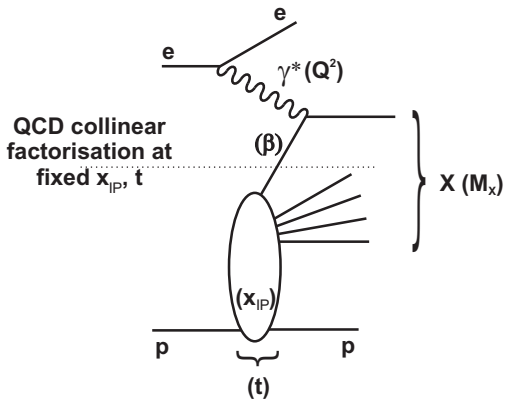

Figure 1: Illustration of the diffractive DIS process $ep \to eXp$ and the kinematic variables used to describe it.

measured at HERA are interpreted in a combined framework, which applies the QCD factorisation theorem to the x and Q^2 dependence and uses a Regge inspired approach to express the dependence on the variables $x_{I\!P}$ and t, which characterise the process at the proton vertex (Fig. 1) [8, 9]. In this framework the data at low $x_{I\!P}$ are well described and DPDFs and a pomeron trajectory intercept are extracted.

In order to describe the data at larger $x_{I\!P}$, it is necessary to include a sub-leading exchange trajectory ($I\!R$), which is consistent with the approximately degenerate trajectories associated with the exchange of ρ, ω, a_2 and f_2 mesons.

2. Selection of diffraction at HERA

In a number of analyses, including [1] and [5], diffractive DIS events were selected on the basis of the presence of a large rapidity gap (LRG) between the leading proton and the remainder of the hadronic final state X (Fig. 1).

In another approach, not considered here, the inclusive DIS sample is decomposed into diffractive and non-diffractive contributions based on their characteristic dependences on the hadronic mass M_x [6]. A complementary way to study diffractive processes is pursued by the direct measurement of the outgoing proton using Forward Proton Spectrometers (FPS) [2, 3, 4, 5]. The FPS method selects events in which the proton scatters elastically, whereas the LRG method does not distinguish the elastic case from proton dissociation to excited systems Y with small masses M_Y. The advantage of the LRG method is that it provides much higher statistics of data than the FPS detectors which have small acceptance. A Very Forward Proton Spectrometer (VFPS), which was operational in the H1 experiment at HERA-2, has much higher acceptance and provides high statistics data [10].

In contrast to the LRG case, the squared four-momentum transfer at the proton vertex t can be reconstructed using the FPS method. The FPS also allows measurements up to higher values of the proton fractional longitudinal momentum loss $x_{I\!P}$ than is possible with the LRG method, extending into regions where the sub-leading trajectory is the dominant exchange. The FPS measurements provide a means of testing in detail whether the variables $x_{I\!P}$ and t associated with the proton vertex can be factorised from the the variables $\beta = x/x_{I\!P}$ and Q^2 describing the hard interaction with the photon. Here β is the longitudinal momentum fraction of the colour singlet carried by the struck quark, x is the Bjorken scaling variable.

The LRG and FPS methods have different systematic uncertainties. The main systematic uncertainties of the LRG method are related to the missing proton and the efficiency of the LRG selection. The LRG data are integrated over $|t| < 1$ GeV^2 and proton dissociative states with low masses M_Y. The FPS systematic uncertainties are dominated by the uncertainties of the HERA beam optics and the position of the detectors relative to the proton beam. The two methods are compared in the H1 and ZEUS publications [3, 5]. The results of the methods are consistent up to a normalisation factor. The LRG events contain about a 20% contribution from proton dissociation, but the ratio of the LRG to FPS cross sections indicates no significant dependence on Q^2, β or $x_{I\!P}$. The ratio of the LRG to FPS cross sections measured in the H1 experiment as a function of Q^2, β and $x_{I\!P}$ for $|t| < 1$ GeV^2 is shown in Fig. 2.

3. The reduced cross section $\sigma_r^{D(4)}$ and test of proton vertex factorisation

A new measurement of the reduced cross section $\sigma_r^{D(4)}(\beta, Q^2, x_{I\!P}, t)$ for the diffractive DIS process $ep \to eXp$ is performed by the H1 Collaboration, using the FPS data collected at HERA-2 [3]. The reduced cross section is related to the diffractive structure functions $F_2^{D(4)}$ and $F_L^{D(4)}$ by

$$\sigma_r^{D(4)} = F_2^{D(4)} - \frac{y^2}{Y_+} F_L^{D(4)}, \qquad (2)$$

where $Y_+ = 1 + (1 - y)^2$, and y is the inelasticity of the process.

The reduced cross section is equal to the diffractive structure function $F_2^{D(4)}(\beta, Q^2, x_{I\!P}, t)$ to a good approximation in the relatively low y region covered by

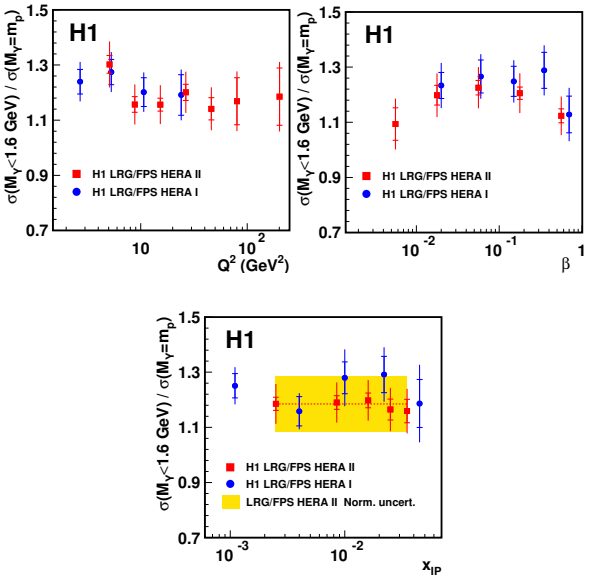

Figure 2: Ratio of the diffractive reduced cross sections measured by H1 with the LRG and FPS methods, shown as a function of Q^2, β and $x_{I\!P}$ for $|t| < 1$ GeV^2.

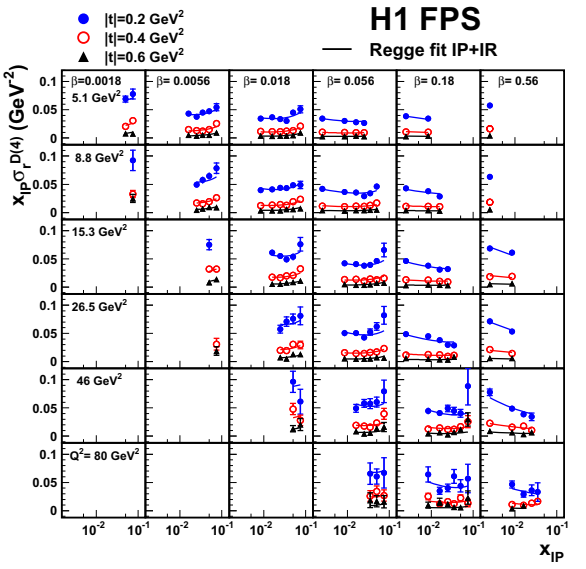

Figure 3: Diffractive reduced cross sections measured by H1, shown as a function of $x_{I\!P}$ for different values of t, β and Q^2. The solid curves represent the results of the phenomenological "Regge" fit to the data, including both pomeron ($I\!P$) and sub-leading ($I\!R$) trajectory exchanges.

the current analysis. The analysed data sample corresponds to an integrated luminosity of 156 pb^{-1}. The data cover the range $0.1 < |t| < 0.7$ GeV^2, $x_{I\!P} < 0.1$ and $4 < Q^2 < 110$ GeV^2. The statistics of DIS events with a leading proton are increased by a factor 20 compared to the previous H1 FPS analysis [2]. The kinematic range of the FPS measurement is extended to higher Q^2. Figure 3 shows $\sigma_r^{D(4)}$ measured by H1 as a function of $x_{I\!P}$ for different t, β and Q^2 values. Previously, the ZEUS Collaboration performed a measurement of $\sigma_r^{D(4)}(\beta, Q^2, x_{I\!P}, t)$ based on an integrated luminosity of 33 pb^{-1} [5]. The ZEUS results are shown in Fig. 4.

To describe the $x_{I\!P}$ and t dependences quantitatively, the structure function $F_2^{D(4)}$ is parameterised by the form

$$F_2^{D(4)} = f_{I\!P}(x_{I\!P}, t) \cdot F_{I\!P}(\beta, Q^2) + n_{I\!R} \cdot f_{I\!R}(x_{I\!P}, t) \cdot F_{I\!R}(\beta, Q^2) \ ;$$

$$f_{I\!P,I\!R}(x_{I\!P}, t) = A_{I\!P,I\!R} \cdot e^{B_{I\!P,I\!R}\, t} / x_{I\!P}^{2\alpha_{I\!P,I\!R}(t)-1} \ ,$$

which assumes a separate proton vertex factorisation of the $x_{I\!P}$ and t dependences from those on β and Q^2 for both the pomeron and the sub-leading exchange [11]. The factors $f_{I\!P}$ and $f_{I\!R}$ correspond to flux factors for the exchanges and are taken from the Regge-motivated functions. The results of the Regge analysis are the intercept and slope of the pomeron trajectory, $\alpha_{I\!P}(t) = \alpha_{I\!P}(0) + \alpha'_{I\!P} t$ and the exponential t-slope parameter $B_{I\!P}$.

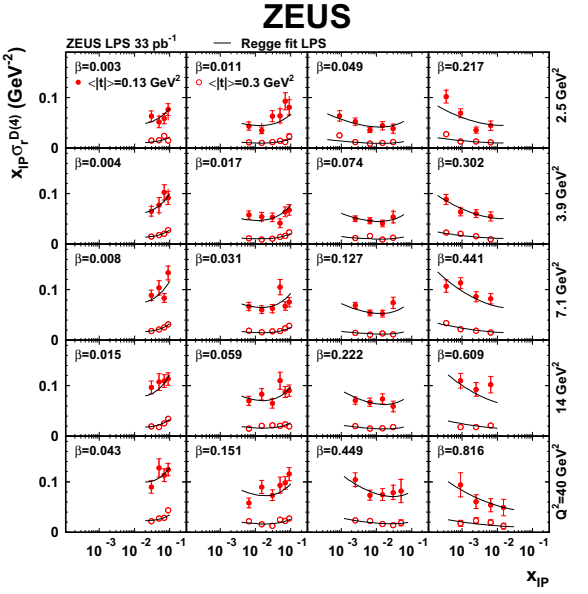

Figure 4: Diffractive reduced cross sections measured by ZEUS, shown as a function of $x_{I\!P}$ for different values of t, β and Q^2.

The normalisation coefficients $F_{I\!R}(\beta, Q^2)$ for the sub-leading exchange in each β and Q^2 bin are taken from a parameterisation of the pion structure function [12]. The fit provides a good description of the $x_{I\!P}$ and t dependences of the data. The result for the intercept $\alpha_{I\!P}(0) \simeq 1.10$ obtained, using the H1 and ZEUS proton

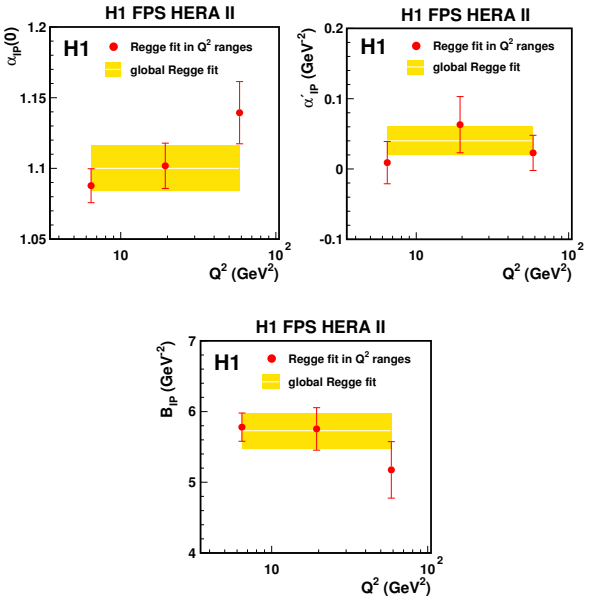

Figure 5: Results from the H1 "Regge" fit for the values of $\alpha_{I\!P}(0)$, $\alpha'_{I\!P}$ and $B_{I\!P}$ in three different ranges of Q^2. The bands show the result and experimental uncertainty from the global fit over the whole Q^2 range.

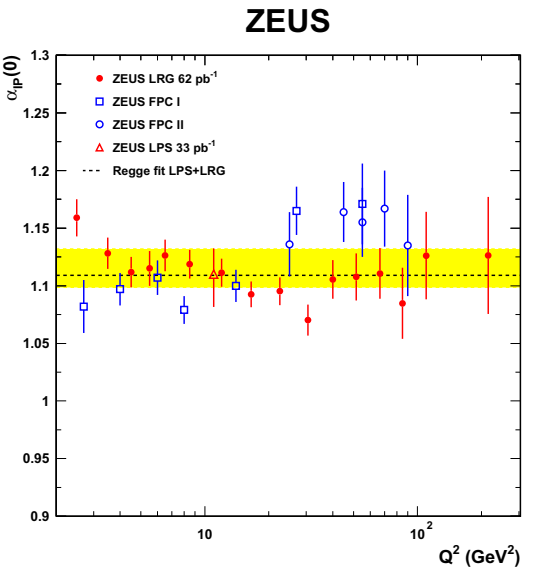

Figure 6: Pomeron intercept $\alpha_{I\!P}(0)$ measured by ZEUS as a function of Q^2.

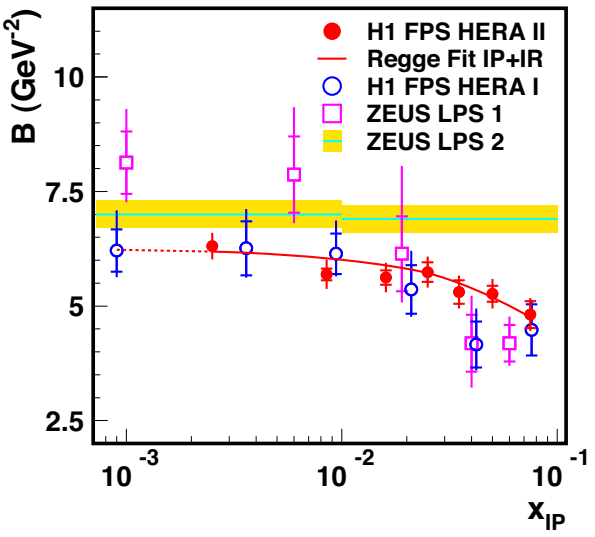

Figure 7: Slope parameter B obtained from a fit of the form $\mathrm{d}\sigma/\mathrm{d}t \propto e^{Bt}$, shown as a function of $x_{I\!P}$. The solid curve represents the results of the "Regge" fit to the H1 data [3], including both pomeron ($I\!P$) and sub-leading ($I\!R$) trajectory exchanges. The previously published H1 [2] and ZEUS results [4, 5] are also shown.

spectrometers, is compatible with that obtained from the data measured using the LRG method [1, 5]. It is also consistent within uncertainties with the pomeron intercept describing soft hadronic scattering, $\alpha_{I\!P}(0) \simeq 1.08$ [13, 14].

In a Regge approach with a single linear exchanged pomeron trajectory, $\alpha_{I\!P}(t) = \alpha_{I\!P}(0) + \alpha'_{I\!P} t$, the exponential t-slope parameter $B_{I\!P}$ of the diffractive cross section is expected to decrease logarithmically with increasing $x_{I\!P}$, an effect which is often referred to as 'shrinkage' of the diffractive peak. The degree of shrinkage depends on the slope of the pomeron trajectory, which is $\alpha'_{I\!P} \simeq 0.25$ GeV^{-2} for soft hadron-hadron scattering at high energies. The H1 and ZEUS data favour a small value of $\alpha'_{I\!P} < 0.1$, as expected in perturbative models of the pomeron [15]. This result is inconsistent with the expected value of $\alpha'_{I\!P}$ from soft hadron-hadron scattering. To check a possible breakdown of proton vertex factorisation implied by a dependence of the $\alpha_{I\!P}(0)$, $\alpha'_{I\!P}$ and $B_{I\!P}$ on Q^2, a modified version of the "Regge" fit of the H1 data is performed in three different ranges of Q^2. The results of the H1 "Regge" fits, shown in Fig. 5, indicate no strong dependence of the pomeron parameters on Q^2. The pomeron intercept $\alpha_{I\!P}(0)$ measured by ZEUS as a function of Q^2 is shown in Fig. 6. The ZEUS results obtained using different methods of the event selection show no significant dependence on Q^2.

The t-dependence of the diffractive cross section is parameterised by an exponential function such that $\mathrm{d}\sigma/\mathrm{d}t \propto e^{Bt}$. Fig. 7 shows the slope parameter B as a function of $x_{I\!P}$ for data averaged over Q^2 and β. The results for B are compared with a parameterisation of the t-dependence from the H1 "Regge" fit to $F_2^{D(4)}$ [3].

At low $x_{I\!P}$ the H1 data are compatible with a constant

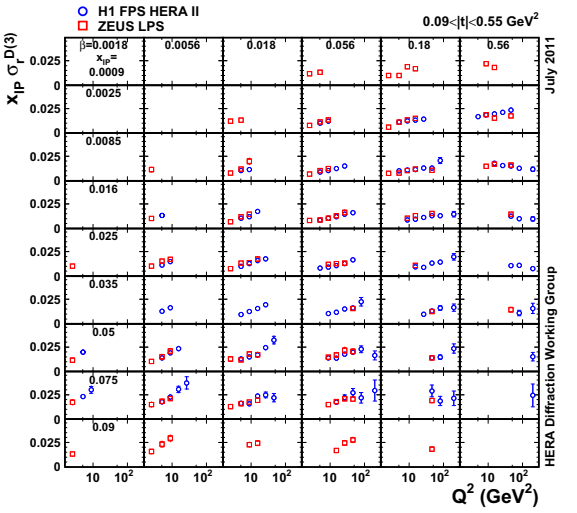

Figure 8: Diffractive reduced cross sections σ_r^D, shown as a function of Q^2 for all measured values of $x_{I\!P}$ and $\beta = x/x_{I\!P}$.

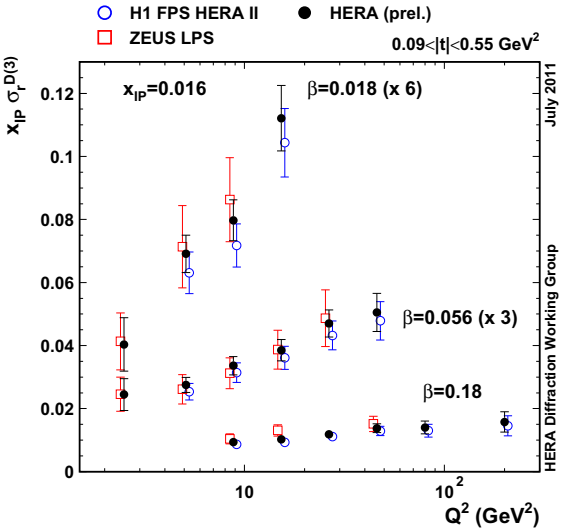

Figure 9: Diffractive reduced cross section σ_r^D, shown as a function of Q^2 for selected values of $x_{I\!P}$ and $\beta = x/x_{I\!P}$. The H1, ZEUS and the combined cross sections (HERA (prel.)) are presented.

slope parameter, $B \simeq 6$ GeV^{-2}. No significant Q^2 or β dependence of the slope parameter B is observed for the data points with $x_{I\!P} \leq 0.025$. A weak decrease of the slope B from 6 GeV^{-2} to below 5 GeV^{-2} is observed towards larger values of $x_{I\!P} > 0.05$, where the contribution from the sub-leading exchange is significant. The recent ZEUS measurement gives $B \simeq 7$ GeV^{-2}, which is found to be independent of $x_{I\!P}$, Q^2 or M_x [5]. The measured value of B is larger than that from "hard" exclusive vector meson production ($ep \to eVp$) [16, 17]. The results of the recent H1 and ZEUS measurements are not consistent at large $x_{I\!P}$, indicating that the systematic uncertainties are underestimated.

In general, the inclusive diffractive data are consistent with "proton vertex" factorisation[11], whereby the dependences on the variables $x_{I\!P}$, t and M_Y, describing the proton vertex, are independent of the variables β and Q^2, which describe the hard interaction with the photon. The dependences on $x_{I\!P}$ and t can then be expressed in terms of an "effective pomeron flux" of a colourless exchange, whilst the β and Q^2 dependences can be interpreted in terms of DPDFs, which describe the partonic structure of that exchange[7].

4. Comparison and combination of diffractive DIS cross sections

The cross sections for diffractive DIS, measured using the H1 and ZEUS proton spectrometers in the range $0.09 < |t| < 0.55$ GeV^2, are found to be in agreement within the experimental uncertainties. A compilation of the results of the two experiments is presented in Fig. 8. The H1 and ZEUS cross sections are combined [18] and are also shown in Fig. 9. Correlations of systematic uncertainties are taken into account by the combination method [19], resulting in an improved precision of the combined cross section. The kinematic range of the combined result is extended in $x_{I\!P}$ and Q^2 compared to that for one experiment.

The H1 and ZEUS Proton Spectrometers select diffractive events over a wide range of $x_{I\!P} < 0.1$, but with limited acceptance. The H1 Very Forward Proton Spectrometer (VFPS), which was operational at HERA-2, has much larger acceptance extending to $t = 0$ over a restricted range of $0.01 \leq x_{I\!P} \leq 0.025$. The first VFPS data on inclusive diffractive DIS based on an integrated luminosity of ~ 100pb^{-1} are released as a preliminary result [10]. The VFPS data agree well with the recent H1 results obtained using the FPS and LRG methods as shown in Fig.10. The finalised VFPS data are expected to provide the best point-to-point precision in the measured $x_{I\!P}$ range.

The diffractive reduced cross section $\sigma_r^{D(3)}$ integrated over $|t| < 1$ GeV^2 is measured differentially in β, Q^2 and $x_{I\!P}$ using the LRG method. The precision achieved using the LRG method is illustrated in Fig. 11, which compares combined H1 data [20] based on a luminosity of 370 pb^{-1} with previously published ZEUS data [5]. The data are in general agreement up to a global factor of $\sim 13\%$, which is at the level expected from normali-

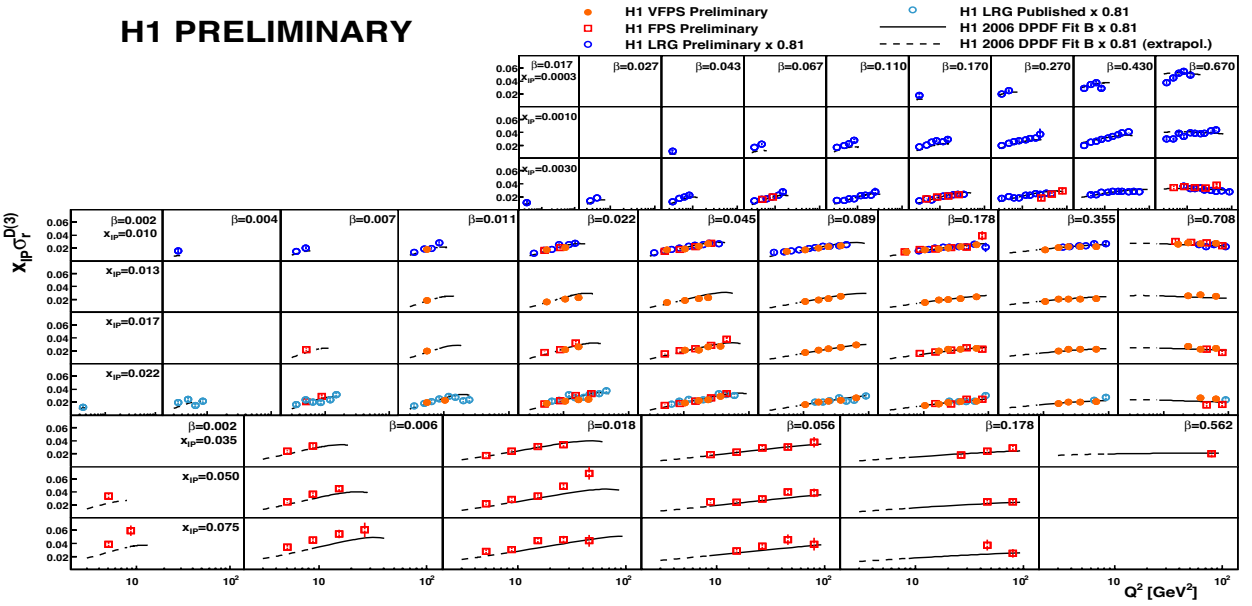

Figure 10: Compilation of the H1 VFPS, FPS and LRG data, showing the Q^2 dependence of the diffractive reduced cross sections at fixed $x_{I\!P}$ and β.

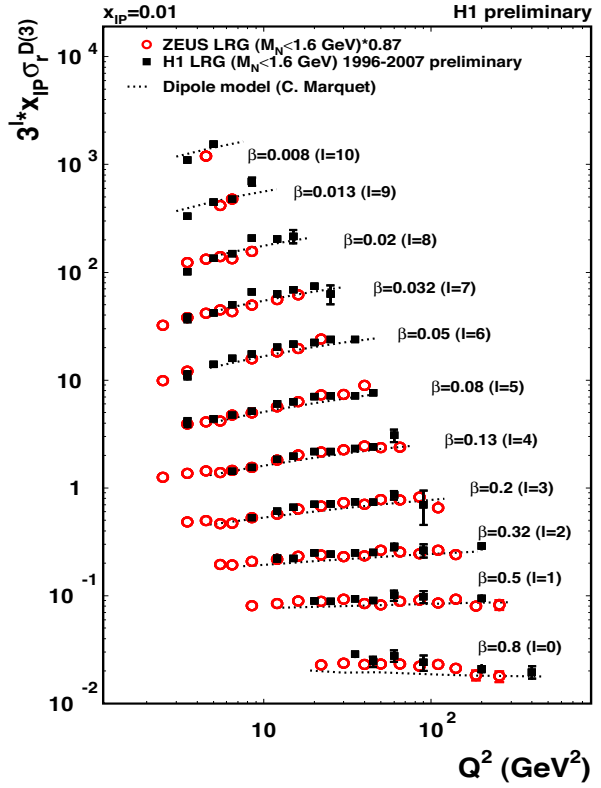

Figure 11: Q^2 dependence of the diffractive reduced cross sections at fixed $x_{I\!P}$ and β, measured by H1 and ZEUS using the LRG method.

sation uncertainties. In a limited range at high β and low $x_{I\!P}$ the H1 and ZEUS results are inconsistent, indicating underestimated systematic uncertainties.

5. QCD analysis of σ_r^D and dijet data in DIS

The β and Q^2 dependences of the inclusive diffractive DIS data are sensitive to the quark singlet and gluon DPDFs. The proton vertex factorisation is assumed in the QCD analysis, i.e. that the DPDFs f_i^D (Eq.1) are parameterised by the form:

$$f_i^D(x, Q^2, x_{I\!P}, t) = f_{I\!P/p}(x_{I\!P}, t) \cdot f_i(\beta = x/x_{I\!P}, Q^2)$$

Parameterising $f_{I\!P/p}(x_{I\!P}, t)$ using a Regge approach, the β and Q^2 dependences of f_i are subjected to a perturbative QCD analysis based on the DGLAP equations in order to obtain DPDFs. The quark singlet density is very closely related to the measured diffractive cross section and is thus well constrained. According to the DGLAP evolution equations, the ln Q^2 derivative contains contributions due to the splittings $g \to q\bar{q}$ and $q \to qg$, convoluted with the diffractive gluon and quark densities, respectively. The derivative is determined almost entirely by the diffractive gluon density. The strong positive ln Q^2 derivatives (scaling violations) for most β values, seen in Fig. 11, imply a large gluon contribution to the DPDFs. At high β, the contribution to the Q^2 evolution from quark splittings $q \to qg$ becomes increas-

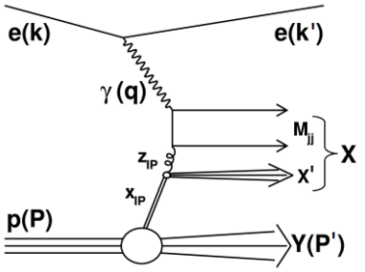

Figure 12: Leading order boson-gluon fusion diagram for dijet production in diffractive DIS.

ingly important, and the derivatives become less sensitive to the gluon density. The DPDFs extracted from the QCD analysis of inclusive diffractive DIS provide important input to final state measurements such as dijet production in DIS [8, 9], which may also provide important additional constraints on the gluon at high fractional momenta. Being dominated by the boson-gluon fusion process $\gamma^* g \to q\bar{q}$ shown in Fig.12, the dijet DIS data are sensitive to the diffractive gluon density directly in contrast to σ_r^D.

This is illustrated in Fig.13, where different ZEUS DPDF parameterisations based on the σ_r^D data are compared with the diffractive dijet DIS cross sections. The dependence of the dijet cross section on $z_{I\!P}$, the dijet fractional momentum, is most sensitive to the gluon DPDF. Combined NLO DGLAP analyses of the σ_r^D and dijet data are performed by the H1 and ZEUS Collaborations. The results of the recent ZEUS QCD analysis [9] based on the high statistics LRG data are presented in Fig. 14. The error bars shown in Fig. 14 represent experimental uncertainties only. The method and DPDF parameterisation are similar to an earlier H1 analysis [8]. The heavy flavours are treated within the general mass variable flavour number scheme [21], whereas H1 used a fixed flavour number scheme. The results of the H1 analysis are presented in Fig. 15, where the error bars include experimental as well as scale uncertainties.

Integrated over β, the gluon density, extracted in the QCD analysis of the ZEUS diffractive DIS data, carries around 60% of the total momentum. The QCD analysis of the H1 diffractive DIS data gives a somewhat higher gluon momentum fraction of 70%, independently of Q^2. The results of the H1 and ZEUS Collaborations are shown in Fig.16. A similar fraction of the total proton momentum is carried by the inclusive gluon density in the low x region where valence quark effects are small [22]. This similarity of the ratio of quarks to gluons in the DPDFs and the inclusive proton

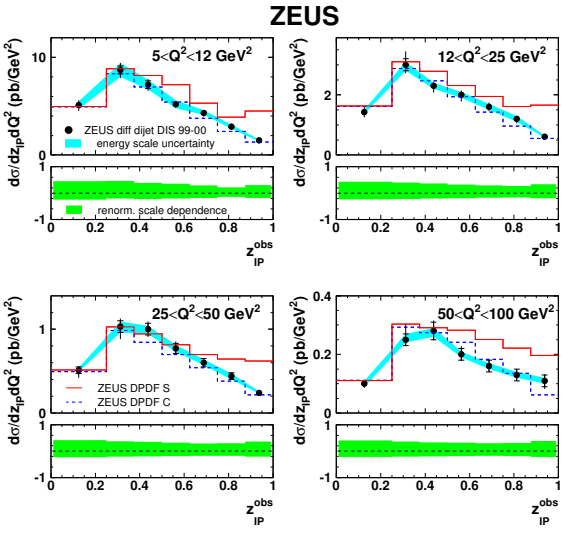

Figure 13: Predictions based on different ZEUS DPDF parameterisations compared with the diffractive dijet DIS data.

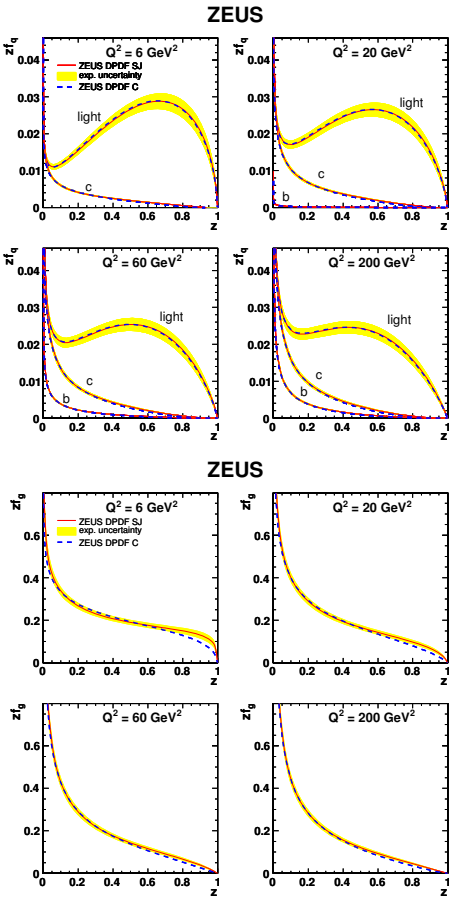

Figure 14: Diffractive quark singlet (top) and gluon densities (bottom) for different values of the hard scale Q^2, extracted from the ZEUS NLO DGLAP analysis of σ_r^D and the dijet DIS data.

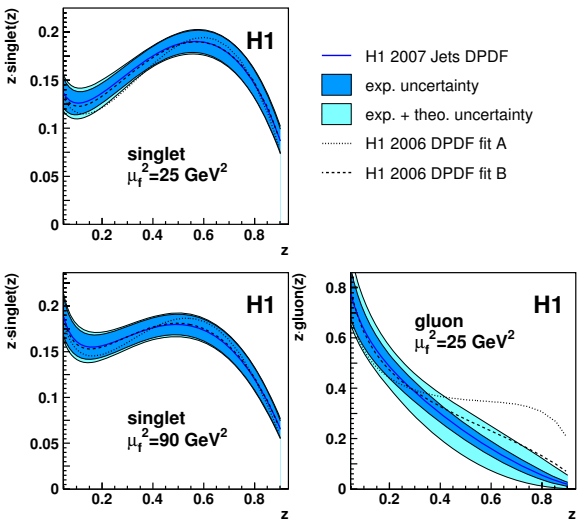

Figure 15: Diffractive quark singlet and gluon densities for different values of the hard scale $\mu_f^2 = Q^2 + p_T^2$, extracted from the H1 NLO DGLAP analysis of σ_r^D and the dijet DIS data.

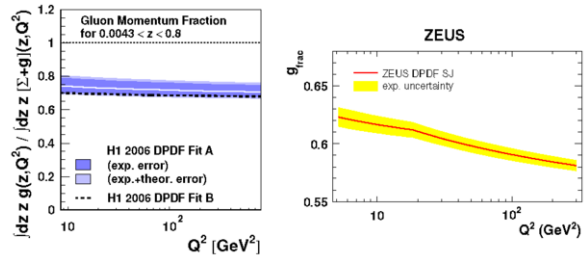

Figure 16: Gluon momentum fraction as a function of Q^2. Results from the H1 and ZEUS QCD analyses are shown.

parton densities is reflected in a ratio of the two cross sections which, to good approximation, is flat as a function of Q^2 at fixed x and $x_{I\!P}$[1, 3].

Predictions from the NLO QCD fits using different DPDFs are compared in Fig.17 with the diffractive reduced cross sections measured by ZEUS using the LRG method. For $Q^2 < 5$ GeV^2 in the ZEUS case and for $Q^2 < 8.5$ GeV^2 in the H1 case, the fits are extrapolated. The normalisation of the ZEUS parameterisation is above that of H1. The H1 DPDFs predict a somewhat stronger Q^2 dependence of the cross section at large β where the predictions are extrapolated. The DPDF results reflect the degree of consistency in the shape and normalisation between the H1 and ZEUS diffractive DIS data.

In recent H1 analyses, dijets are selected in events with a leading proton tagged in the FPS and VFPS [23, 24], allowing new regions of phase space to be explored in

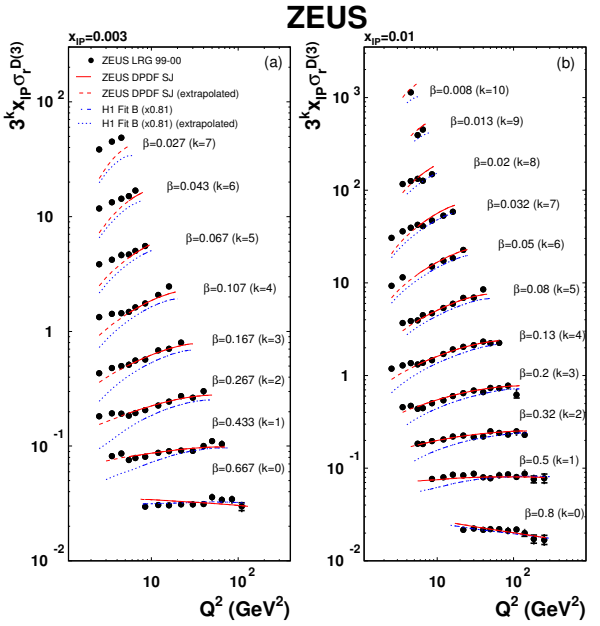

Figure 17: Q^2 dependence of the diffractive reduced cross sections at fixed $x_{I\!P}$ and β, measured by ZEUS using the LRG method. Predictions from the H1 and ZEUS QCD fits are shown.

which there are jets in rapidity beyond the LRG range. These selections may enhance "hard" pomeron contributions [25], where all of the exchanged momentum enters the hard scattering ($z_{I\!P} \simeq 1$), and the jets are produced exclusively. However, these data are well described by NLO DPDF predictions, as illustrated in Fig.18, suggesting that the "hard" pomeron contribution has a relatively small cross section. DPDF predictions at leading order (LO), also shown in Fig.18, underestimate the cross sections by a factor of ~ 2.

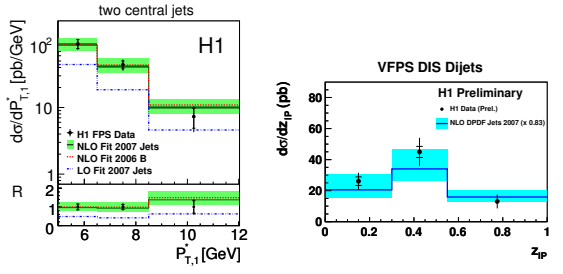

Figure 18: Differential cross sections for diffractive dijet production in DIS, measured by the H1 FPS and VFPS as a function of p_T^* of the leading jet and $z_{I\!P}$ compared to NLO predictions based on different sets of DPDFs.

The measured dijet cross sections for two dijet event topologies are compared in Fig. 19 with Monte Carlo models based on leading order matrix elements and par-

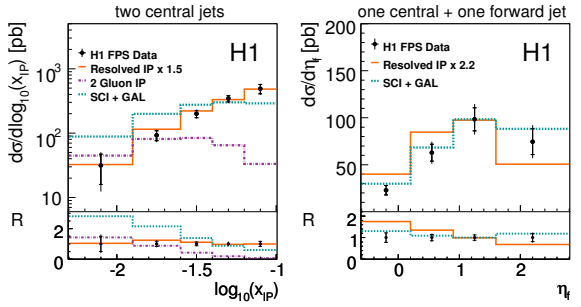

Figure 19: Differential cross sections for diffractive dijet production in DIS, measured by the H1 FPS as a function of $\log_{10} x_{\mathbb{P}}$ and $z_{\mathbb{P}}$ compared to predictions of LO Monte Carlo models.

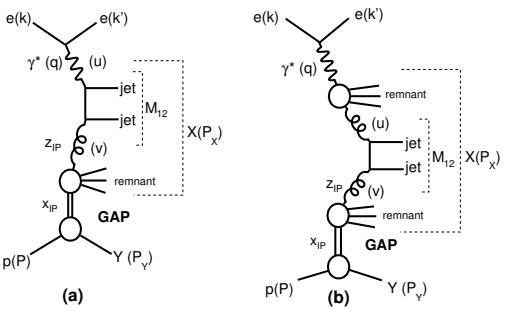

Figure 20: Illustration of dijet production via direct photon (a) and resolved photon (b) processes.

ton showers. The resolved pomeron model [11], based on proton vertex factorisation and the DPDF set H1 2006 Fit B [1], describes the shape of the cross sections well, but the normalisation of the cross sections is too low. This suggests that contributions from higher order processes are important in order to describe the measured dijet cross sections. The SCI+GAL model, based on soft colour interactions of final state partons [26], is able to reproduce the normalisation of the cross section for both dijet topologies presented after tuning the probability of soft colour interactions. The dependence of the diffractive dijet cross section on $x_{\mathbb{P}}$ and $z_{\mathbb{P}}$ is able to distinguish between the models. The SCI+GAL model and 'hard' two gluon pomeron model [25] fail to describe the shape of the distributions of the diffractive variables, while the resolved pomeron model describes the shape of these distributions well.

6. Diffractive dijets in photoproduction

Measurements of diffractive dijet photoproduction provide tests of QCD factorisation, DPDFs extracted in diffractive DIS, and they allow us to estimate "absorptive" effects of multiple interactions which occur in the presence of beam remnants. In dijet photoproduction the hard scale is defined by E_T, the transverse energy of jets, because $Q^2 \sim 0$. QCD collinear factorisation is expected to be valid in direct processes with point-like photons, but broken in processes with resolved photons, where the photon interacts via its partonic structure, and secondary interactions between the photon and proton remnants may fill the rapidity gap [27]. The two processes can be separated using the variable x_γ, which corresponds to the parton longitudinal momentum fraction of the photon entering the hard sub-process. Resolved photon processes correspond to $x_\gamma < 1$, whereas direct photon processes to $x_\gamma \simeq 1$. Resolved and direct photon processes of dijet production are illustrated in Fig.20. The ratio of the dijet photoproduction cross sections of ZEUS and H1 to various NLO calculations are shown in Figs. 21 and 22. The recent H1 data [28]

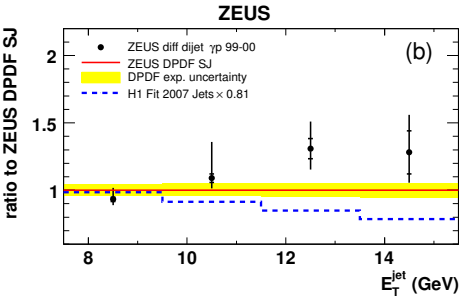

Figure 21: Ratio of the differential cross sections for diffractive dijet photoproduction measured by ZEUS to the NLO QCD calculations based on DPDFs extracted from diffractive DIS.

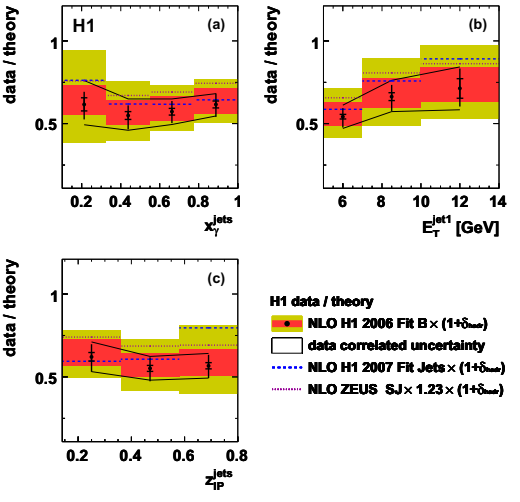

Figure 22: Ratio of the differential cross sections for diffractive dijet photoproduction measured by H1 to the NLO QCD calculations based on DPDFs extracted from diffractive DIS.

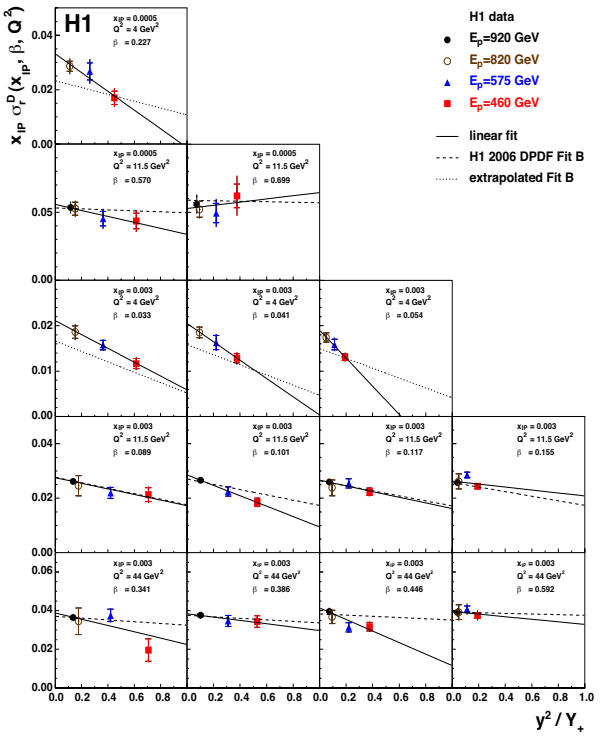

Figure 23: Diffractive reduced cross sections σ_r^D as a function of y^2/Y_+ at fixed Q^2, $x_{I\!P}$ and β. The linear fits to the data are presented as a solid line, the slope of which gives the value of F_L^D.

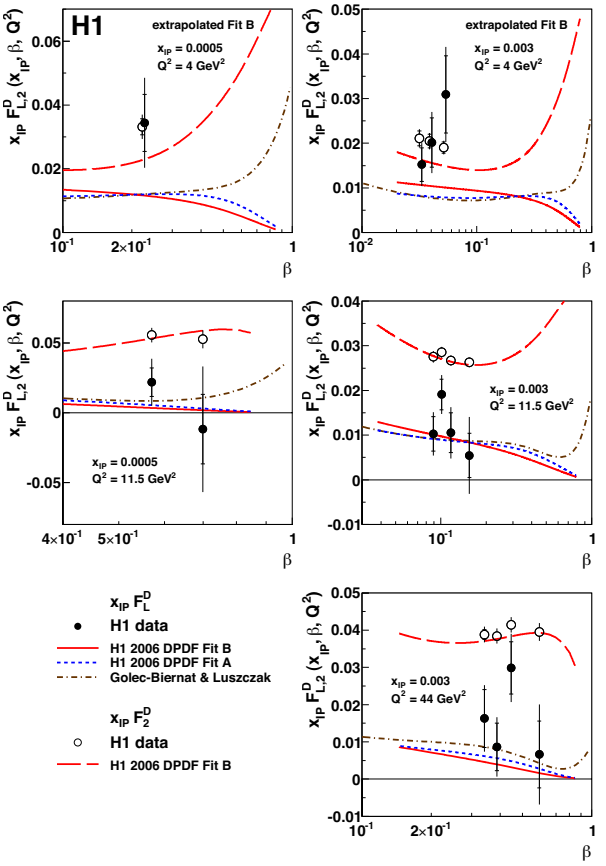

Figure 24: Diffractive structure functions F_L^D and F_2^D as a function of β at fixed Q^2 and $x_{I\!P}$. Predictions based on NLO QCD fits and of a colour dipole model are shown as curves.

suggest a suppression of the photoproduction data by a factor 0.6 ± 0.2 relative to the NLO QCD predictions, with no significant difference between resolved and direct processes. The ZEUS results for larger jet transverse energies [9] suggest no suppression, but also do not show the expected difference between resolved and direct photon enhanced samples. A possible explanation for the apparent discrepancy between the two experiments is a rising dependence of the data-to-theory ratio on the jet transverse energy. The ZEUS measurement is performed for $E_T^{jet} > 7.5$ GeV, whereas H1 measured for $E_T^{jet} > 5$ GeV. In contrast to theoretical expectations [27, 29], the ratios of data to theory measured by both collaborations have at most a weak dependence on x_γ. These issues are partially resolved by recent predictions in which a more detailed treatment of the point-like photon structure is introduced [30].

7. Diffractive longitudinal structure function F_L^D

Similarly to the case of inclusive DIS, the diffractive longitudinal structure function F_L^D provides a complementary measurement of the diffractive gluon density. To extract F_L^D, the diffractive reduced cross sections are measured by the H1 Collaboration at the proton energies of 460, 575 and 920 GeV in the range of photon virtuality of $4 \le Q^2 \le 44$ GeV^2. The data are combined with the previously published measurement at 820 GeV [1]. A linear fit is performed to the reduced cross section as a function of y^2/Y_+ (Eq. 2) to extract the diffractive longitudinal structure function F_L^D and the structure function F_2^D as shown in Fig. 23. The results of the fit for F_L^D and F_2^D are shown in Fig. 24 and are compared with predictions derived from leading twist NLO QCD fits to the previous H1 LRG data [1]. The F_L^D measurement provides an additional test of the DPDFs. The data are compatible with the H1 DPDF fits as well as with a model which is based on the colour dipole approach and which includes a higher twist contribution at high β [31].

The ratio R^D of diffractive cross sections for longitudinally to transversely polarised photons is measured

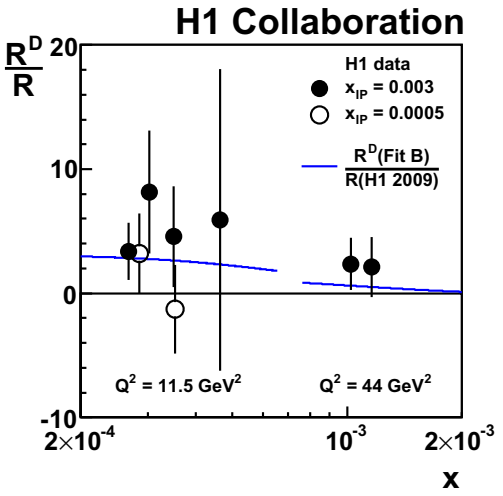

Figure 25: Ratio R^D/R as a function of x at fixed Q^2 and $x_{I\!P}$. The data are compared with the predicted ratio using the H1 DPDF Fit B / H1 PDF 2009 Fit (solid line).

in the same kinematic range as F_L^D. The ratio suggests that the cross sections for the two polarisation states of the photon are of comparable size. The ratio of R^D to R for diffractive and inclusive scattering, shown in Fig. 25, indicates that the longitudinally polarised photon cross section plays a larger role in diffractive than in inclusive processes. The R^D and R^D/R results are well reproduced by the predictions based on the H1 DPDF Fit B and the H1 PDF 2009 inclusive PDF set [22].

8. Conclusions

Results on diffractive cross sections in DIS are in general agreement between the H1 and ZEUS experiments and between the two methods of diffractive event selection. The cross sections for processes with a leading proton in the final state and with a large gap in the rapidity distribution of the final state hadrons are consistent, after applying a correction for the proton dissociation contribution in the later process. The first combination of the leading proton cross sections measured by the H1 and ZEUS Collaborations improves the precision of the measurement. The H1 and ZEUS data support the hypothesis of proton vertex factorisation, which states that the cross section dependences on the variables which describe soft process at the proton vertex are independent of the variables of the hard scattering process at the photon vertex. The PDF structure of the diffractive exchange is studied in NLO DGLAP analyses of diffractive DIS data. The diffractive PDFs are dominated by a hard gluon density, which successfully describes hard dijet final states in diffractive DIS and the longitudinal diffractive structure function F_L^D. The rapidity gap survival probability derived from predictions of the NLO diffractive parton densities for hard dijet photoproduction data are similar for direct and resolved photon interactions as observed by H1 and ZEUS. H1 finds an overall suppression factor of around 0.6 for dijet photoproduction, whereas the cross sections measured by ZEUS for larger jet transverse energies suggest no suppression.

References

[1] A. Aktas *et al.* [H1 Collaboration], Eur. Phys. J. C 48 (2006) 715 [hep-ex/0606004].
[2] A. Aktas *et al.* [H1 Collaboration], Eur. Phys. J. C 48 (2006) 749 [hep-ex/0606003].
[3] F.D. Aaron *et al* [H1 Collaboration], Eur. Phys. J. C 71 (2010) 1578 [arXiv:1010.1476].
[4] S. Chekanov *et al.* [ZEUS Collaboration], Eur. Phys. J. C 38 (2004) 43 [hep-ex/0408009].
[5] S. Chekanov *et al.* [ZEUS Collaboration], Nucl. Phys. B 816 (2009) 1 [hep-ex/0408009].
[6] S. Chekanov *et al.* [ZEUS Collaboration], Nucl. Phys. B 800 (2008) 1.
[7] J. Collins, Phys. Rev. D 57 (1998) 3051 [Erratum-ibid. D 61 (2000) 019902].
[8] A. Aktas *et al.* [H1 Collaboration], JHEP 0710:042 (2007) [arXiv:0708.3217].
[9] S. Chekanov *et al.* [ZEUS Collaboration], Nucl. Phys. B 831 (2010) 1.
[10] H1 Collaboration, *F2D3 with VFPS*, presented at DIS-2010, `H1prelim-10-014` (2010).
[11] G. Ingelman, P. Schlein, Phys. Lett. B 152 (1985) 256.
[12] J. Owens, Phys. Rev. D 30 (1984) 943.
[13] G. Jaroszkiewicz, P. Landshoff, Phys. Rev. D 10 (1974) 170.
[14] A. Donnachie, P.V. Landshoff, Nucl. Phys. B 231 (1984) 189; A. Donnachie, P.V. Landshoff, Phys. Lett. B B296 (1992) 227 [hep-ph/9209205]; J. Cudell, K. Kang, S. Kim, Phys. Lett. B 395 (1997) 311 [hep-ph/9601336].
[15] J. Bartels, H. Kowalski, Eur. Phys. J. C 19 (2001) 693 [hep-ph/0010345].
[16] S. Chekanov *et al.* [ZEUS Collaboration], Eur. Phys. J. C 24 (2002) 345 [hep-ex/0201043].
[17] A. Aktas *et al.* [H1 Collaboration], Eur. Phys. J. C 46 (2006) 585 [hep-ex/0510016]; F.D. Aron *et al.* [H1 Collaboration], JHEP 1005 (2010) 032 [arXiv:0910.5831].
[18] H1 and ZEUS Collaborations: *Combined Measurement of the Inclusive Diffractive Cross Sections at HERA* presented at EPS-2011, `H1-preliminary-11-111`, `ZEUS-preliminary-11-011`.
[19] A. Glazov, AIP Conf. Proc. 792 (2005) 237.
[20] H1 Collaboration, *F2D3 with rapidity gap*, presented at DIS-2010, `H1prelim-10-011` (2010).
[21] R. Thorne, R. Roberts, Phys. Rev. B 57 (1998) 6871 [hep-ph/9709442].
[22] F.D. Aron *et al.* [H1 Collaboration], Eur. Phys. J. C 64 (2009) 561 [arXiv:0904.3513].

[23] F.D. Aron *et al.* [H1 Collaboration], DESY 11-166 [arXiv:1111.0584].
[24] H1 Collaboration, *Dijet production in diffractive deep inelastic scattering using the VFPS at HERA*, presented at DIS-2011, `H1prelim-11-013` (2011).
[25] J. Bartels, C. Ewerz, H. Lotter, M. Wuüsthoff, M. Diehl, [hep-ph/9609239].
J. Bartels, H. Jung, M. Wüsthoff, Eur. Phys. J. C 11 (1999) 111 [hep-ph/9903265].
[26] A. Edin, G. Ingelman, J. Rathsman, Phys. Lett. B 366 (1996) 371 [hep-ph/9508386], Z. Phys. C 75 (1997) 57 [hep-ph/9605281].
[27] A. Kaidalov *et al.*, Phys. Lett. B567 (2003) 61 [hep-ph/0306134].
[28] F.D. Aron *et al.* [H1 Collaboration], Eur. Phys. J. C 70 (2010) 15 [arXiv:1006.0946].
[29] M. Klasen, G. Kramer, Mod. Phys. Lett. A 23 (2008) 1885 [hep-ph/0806.2269].
[30] A. Kaidalov *et al.*, Eur. Phys. J. C 66 (2010) 373 [hep-ph/0911.3716].
[31] K.J. Golec-Biernat, A. Luszczal, Phys. Rev. D 76 (2007) 114014 [arXiv:0704.1608].